LA-1393

[redacted]

c.3



# LOS ALAMOS SCIENTIFIC LABORATORY

OF THE

UNIVERSITY OF CALIFORNIA

CONTRACT W-7405-ENG. 36 WITH

U. S. ATOMIC ENERGY COMMISSION



UNCLASSIFIED

[redacted]

[redacted] UNCLASSIFIED

LOS ALAMOS SCIENTIFIC LABORATORY

of the

UNIVERSITY OF CALIFORNIA

Report written:
March 25, 1952

LA-1393

This document consists of 51 pages

[redacted] Series A





# THEORETICAL EQUATION OF STATE FOR DETONATION PRODUCTS OF SOLID EXPLOSIVES. II. DETONATION VELOCITIES AND CHAPMAN-JOUGET P, V, AND T FOR RDX ASSUMING A FIXED PRODUCT COMPOSITION

by

Wm. W. Wood

W. Fickett

[redacted]
Classification changed
by
Report Library
12-18-55



[redacted] UNCLASSIFIED

[redacted]

UNCLASSIFIED

Distributed: APR 4 1952

LA-1393

| | |
|---|---|
| Washington Document Room | 1 - 7 |
| J R. Oppenheimer | 8 |
| Los Alamos Report Library | 9 - 30 |



[redacted] INFORMATION



UNCLASSIFIED

## ABSTRACT

Detonation velocities computed for RDX by use of a free volume equation of state for mixtures are compared with existing experimental data, and certain possible implications of the comparison are discussed. Numerical tables of the Lennard-Jones and Devonshire equation of state in the high temperature-high density region are presented.



## ACKNOWLEDGMENT

Shortly before the preparation of this report we were able to discuss the subject matter with Prof. J. G. Kirkwood, to whom we are grateful for his advice and inspiration.

[redacted]

# A Theoretical Equation of State for Detonation Products of Solid Explosives. II. Detonation Velocities and Chapman-Jouget P, V, and T for RDX Assuming a Fixed Product Composition

## Introduction:

This is an interim report on the theoretical aspects of the current equation of state program in GMX. It is the second member of the series begun with the report by Zevi W. Salsburg[1]. A revised and corrected version of this latter report will be issued shortly.

The numerical calculations presented here supplant those of Section D of reference (1). As mentioned in the latter the available tables were not well adapted to detonation calculations, and the calculations reported there were unavoidably inaccurate. Section I describes briefly the extension of the equation of state tables which was so evidently needed. Section 2 is devoted to the present numerical procedure, while Section 3 describes the results obtained for the explosive RDX. In Section 4 these results are discussed and our future program outlined.

---

[1] "An Equation of State for Fluid Mixtures," dated September 4, 1951, issued by GMX-2.



[redacted]

Section 1.

## Tables Of The Lennard-Jones And Devonshire Equation Of State At High Temperatures And Densities

The Lennard-Jones and Devonshire equation of state has been presented in tabular form by Wentorff, et al[2]. These tables are not sufficient for our purposes for two reasons: They do not extend to sufficiently low values of the reduced volume, and the intervals in both reduced temperature and reduced volume are unsatisfactory for interpolation in the region of interest to us.

Accordingly, we have prepared a tabulation of the equation of state which extends to lower reduced volumes and covers the region of interest with considerably finer intervals in reduced temperature and more regular intervals in reduced volume. The potential of intermolecular force was the same as that used in reference (2), $V(r) = 4\epsilon^*\left[\left(\frac{r_0}{r}\right)^{12} - \left(\frac{r_0}{r}\right)^{6}\right]$. The calculations were quite similar to those described there, and were carried out on an International Business Machines Corporation Model II CPEC combination. The numerical integrations were carried out with Simpson's rule and a nominal 64 to 72 values of the integrand. Shortening of the range of integration was carried out as required so that the number of non-negligible values was always at least two-thirds of the nominal

---

[2]R. H. Wentorff, R. J. Buehler, J. O. Hirschfelder, and C. F. Curtiss, J. Chem. Phys. 18, 1484 (1950)

number. Thus these results are somewhat more accurate than those of Wentorff, et al, who state that they used Simpson's rule with 15 to 30 non-negligible values of the integrand. A rough estimate of the error involved in the numerical evaluation of the integrals was obtained by comparing the results with those obtained by using Simpson's rule with half the original number of points. The number of figures to be included in the tabular entries was decided on the basis of this comparison. Although the last figure in each entry is thought to have some significance, it is not necessarily a "significant figure" in the strict sense.

The results of the calculation are presented in Tables I - VI. The reduced volume and temperature are defined as follows: $T = \frac{v}{v^*}$ and $\theta = \frac{kT}{\epsilon^*}$, where $v^* = N_A r_0^3$ ($N_A$ being Avogadro's number) and $\epsilon^*$ are the molecular parameters defining the Lennard-Jones potential of intermolecular force. The symbols G, $g_l$, and $g_m$ represent integrals needed for the evaluation of the compressibility factor $\mathcal{H} = \frac{pv}{NkT}$, the reduced internal energy of gas imperfection $\mathcal{E}' = \frac{E'}{N\epsilon^*}$, and the reduced entropy of gas imperfection $S'/Nk$. Precise definitions of and expressions for these quantities may be found in reference (2).[3]

To facilitate interpolation, tables of $\mathcal{H}\theta$, $\log(\mathcal{H}-1)$ and $\log \mathcal{E}'$ were prepared. With these, five-point interpolation in $T$ and three-point interpolation in $\theta$ gave satisfactory results.

---

[3]It should be noted that Eq. (21) of reference (2) is incorrect. The correct expression for the entropy is

(Continued on Page 7)



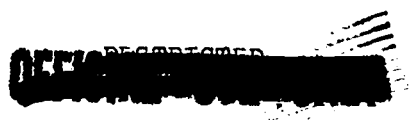

[redacted]

---

$$S = S^\circ(T) - N_A k \log (NkT/v_0^*) + N_A k \log (v/v^*)$$
$$+ S'(v,T) + N_A k \log (\sigma/e) + N_A kT \frac{\partial \log \sigma}{\partial T}$$

$$S'(v,T) = (12 N_A \epsilon^*/T)\left[(v^*/v)^4 (g_L/G) - 2 (v^*/v)^2 (g_m/G)\right]$$
$$+ Nk \log (G/G_\infty)$$

$$G_\infty = \lim_{v \to \infty} G = (2\sqrt{2}\,\pi)^{-1}$$

The parameter $\sigma$ has been precisely defined by Kirkwood, J. Chem. Phys. 18, 380 (1950). It has the property:

$$\lim_{v \to \infty} \sigma = e$$
$$\lim_{v \to 0} \sigma = 0$$

each limit presumably being approached with zero slope.

Thus the error in Eq. (21) of reference (2) is approximately $(-N_A k)$ in the region of present interest, where $\sigma$ is probably close to one.



[redacted]

Table I. A tabulation of G

| θ \ T | .30 | .35 | .40 | .45 | .50 |
|---|---|---|---|---|---|
| 20 | 1.3974 (-5) | 3.5436 (-5) | 7.8929 (-5) | 1.5865 (-4) | 2.9305 (- |
| 30 | 2.5404 (-5) | 6.3[illegible]53 (-5) | 1.4045 (-4) | 2.7771 (-4) | 5.0264 (- |
| 40 | 3.8708 (-5) | 9.6496 (-5) | 2.0983 (-4) | 4.0887 (-4) | 7.2740 (- |
| 50 | 5.3540 (-5) | 1.3245 (-4) | 2.8498 (-4) | 5.4811 (-4) | 9.6080 (- |
| 60 | 6.9688 (-5) | 1.7110 (-4) | 3.6454 (-4) | 6.9284 (-4) | 1.19891(- |
| 70 | 8.6961 (-5) | 2.1199 (-4) | 4.4753 (-4) | 8.4152 (-4) | 1.43935(- |
| 80 | 1.0522 (-4) | 2.5478 (-4) | 5.3326 (-4) | 9.9289 (-4) | 1.68059(- |
| 90 | 1.2437 (-4) | 2.9919 (-4) | 6.2108 (-4) | 1.14608 (-3) | 1.92159(- |
| 100 | 1.4432 (-4) | 3.4500 (-4) | 7.1075 (-4) | 1.30046 (-3) | 2.1612 (- |
| 110 | 1.6498 (-4) | 3.9203 (-4) | 8.0182 (-4) | 1.45555 (-3) | 2.3997 (- |
| 120 | 1.8630 (-4) | 4.4012 (-4) | 8.9403 (-4) | 1.61097 (-3) | 2.6362 (- |
| 130 | 2.0821 (-4) | 4.8914 (-4) | 9.8713 (-4) | 1.76643 (-3) | 2.8707 (- |
| 140 | 2.3067 (-4) | 5.3898 (-4) | 1.08095 (-3) | 1.92172 (-3) | 3.1029 (- |
| 150 | 2.5362 (-4) | 5.8953 (-4) | 1.17533 (-3) | 2.07666 (-3) | 3.3327 (- |

Note: The number in parentheses is the power of 10 by which the entry is to be multiplied.

Table I. (continued)

| θ \ T | .55 | .60 | .65 | .70 | .80 |
|---|---|---|---|---|---|
| 20 | 5.0377 (-4) | 8.1403 (-4) | 1.24644 (-3) | 1.8205 (-3) | 3.4501 |
| 30 | 8.4415 (-4) | 1.32997 (-3) | 1.98348 (-3) | 2.8203 (-3) | 5.0760 |
| 40 | 1.19892 (-3) | 1.85204 (-3) | 2.7068 (-3) | 3.7754 (-3) | 6.5537 |
| 50 | 1.55874 (-3) | 2.3690 (-3) | 3.4085 (-3) | 4.6825 (-3) | 7.9083 |
| 60 | 1.91891 (-3) | 2.8770 (-3) | 4.0857 (-3) | 5.5442 (-3) | 9.1606 |
| 70 | 2.2762 (-3) | 3.3738 (-3) | 4.7385 (-3) | 6.3641 (-3) | 1.03269 |
| 80 | 2.6299 (-3) | 3.8586 (-3) | 5.3679 (-3) | 7.1462 (-3) | 1.14198 |
| 90 | 2.9787 (-3) | 4.3513 (-3) | 5.9753 (-3) | 7.8941 (-3) | 1.24492 |
| 100 | 3.3222 (-3) | 4.7920 (-3) | 6.56201 (-3) | 8.6107 (-3) | 1.34231 |
| 110 | 3.6602 (-3) | 5.2412 (-3) | 7.12946 (-3) | 9.2991 (-3) | 1.43481 |
| 120 | 3.9924 (-3) | 5.6793 (-3) | 7.67894 (-3) | 9.9615 (-3) | 1.52294 |
| 130 | 4.3191 (-3) | 6.1068 (-3) | 8.21164 (-3) | 1.06001 (-2) | 1.60715 |
| 140 | 4.6401 (-3) | 6.5241 (-3) | 8.72865 (-3) | 1.12168 (-2) | 1.68783 |
| 150 | 4.9556 (-3) | 6.9317 (-3) | 9.23098 (-3) | 1.18133 (-2) | 1.76529 |

Table I. (continued)

| θ \ T | .90 | 1.00 | 1.10 | 1.20 | 1.30 |
|---|---|---|---|---|---|
| 20 | 5.7596 (-3) | 8.72641 (-3) | 1.22723 (-2) | 1.62921 (-2) | 2.06759 ( |
| 30 | 8.08891 (-3) | 1.17704 (-2) | 1.59936 (-2) | 2.06249 (-2) | 2.55424 ( |
| 40 | 1.01207 (-2) | 1.43411 (-2) | 1.90591 (-2) | 2.41280 (-2) | 2.94228 ( |
| 50 | 1.19315 (-2) | 1.65830 (-2) | 2.16889 (-2) | 2.70963 (-2) | 3.26809 ( |
| 60 | 1.35709 (-2) | 1.85805 (-2) | 2.40040 (-2) | 2.96860 (-2) | 3.55046 ( |
| 70 | 1.50726 (-2) | 2.03877 (-2) | 2.60793 (-2) | 3.19914 (-2) | 3.80053 ( |
| 80 | 1.64611 (-2) | 2.20419 (-2) | 2.79646 (-2) | 3.40741 (-2) | 4.02550 ( |
| 90 | 1.77543 (-2) | 2.35698 (-2) | 2.96952 (-2) | 3.59770 (-2) | 4.23034 ( |
| 100 | 1.89661 (-2) | 2.49913 (-2) | 3.12969 (-2) | 3.77313 (-2) | 4.41861 ( |
| 110 | 2.01075 (-2) | 2.63220 (-2) | 3.27894 (-2) | 3.93603 (-2) | 4.59299 ( |
| 120 | 2.11870 (-2) | 2.75739 (-2) | 3.41879 (-2) | 4.08823 (-2) | 4.75552 ( |
| 130 | 2.22120 (-2) | 2.87568 (-2) | 3.55046 (-2) | 4.23114 (-2) | 4.90782 ( |
| 140 | 2.31881 (-2) | 2.98787 (-2) | 3.67494 (-2) | 4.36592 (-2) | 5.05117 ( |
| 150 | 2.41205 (-2) | 3.09460 (-2) | 3.79304 (-2) | 4.49352 (-2) | 5.18662 ( |

Table II. A tabulation of $g_L$

| θ \ T | .30 | .35 | .40 | .45 | .50 |
|---|---|---|---|---|---|
| 20 | 2.915 (-7) | 1.5736 (-6) | 5.2184 (-6) | 1.6717 (-5) | 4.6548 (-5 |
| 30 | 7.890 (-7) | 3.6668 (-6) | 1.3653 (-5) | 4.2604 (-5) | 1.1501 (-4 |
| 40 | 1.5919 (-6) | 7.3004 (-6) | 2.6693 (-5) | 8.1459 (-5) | 2.1441 (-4 |
| 50 | 2.7353 (-6) | 1.2336 (-5) | 4.4543 (-5) | 1.3329 (-4) | 3.4339 (-4 |
| 60 | 4.2442 (-6) | 1.8981 (-5) | 6.7288 (-5) | 1.9791 (-4) | 5.0042 (-4 |
| 70 | 6.1402 (-6) | 2.7177 (-5) | 9.4943 (-5) | 2.7491 (-4) | 6.8395 (-4 |
| 80 | 8.4406 (-6) | 3.6964 (-5) | 1.2748 (-4) | 3.6393 (-4) | 8.9258 (-4 |
| 90 | 1.1157 (-5) | 4.8375 (-5) | 1.6487 (-4) | 4.5455 (-4) | 1.1250 (-3 |
| 100 | 1.4206 (-5) | 6.1422 (-5) | 2.0699 (-4) | 5.7638 (-4) | 1.3786 (-3 |
| 110 | 1.7687 (-5) | 7.6108 (-5) | 2.5380 (-4) | 6.9901 (-4) | 1.6540 (-3 |
| 120 | 2.1915 (-5) | 9.2432 (-5) | 3.0519 (-4) | 8.3210 (-4) | 1.9493 (-3 |
| 130 | 2.7392 (-5) | 1.1038 (-4) | 3.6108 (-4) | 9.7527 (-4) | 2.2637 (-3 |
| 140 | 3.1324 (-5) | 1.2996 (-4) | 4.2137 (-4) | 1.1288 (-3) | 2.5962 (-3 |
| 150 | 3.6714 (-5) | 1.5113 (-4) | 4.8598 (-4) | 1.2906 (-3) | 2.9459 (-3 |

Table II. (continued)

| θ \ τ | .55 | .60 | .65 | .70 | .80 |
|---|---|---|---|---|---|
| 20 | 1.1524 (-4) | 2.5793 (-4) | 5.2951 (-4) | 1.0086 (-3) | 3.0394 ( |
| 30 | 2.7506 (-4) | 5.9368 (-4) | 1.1759 (-3) | 2.1571 (-3) | 6.0754 ( |
| 40 | 4.9901 (-4) | 1.0485 (-3) | 2.0175 (-3) | 3.6121 (-3) | 9.7168 ( |
| 50 | 7.8180 (-4) | 1.6056 (-3) | 3.0279 (-3) | 5.3167 (-3) | 1.38230 ( |
| 60 | 1.1188 (-3) | 2.2554 (-3) | 4.1820 (-3) | 7.2302 (-3) | 1.83034 ( |
| 70 | 1.5035 (-3) | 2.9873 (-3) | 5.4618 (-3) | 9.3229 (-3) | 2.30952 ( |
| 80 | 1.9344 (-3) | 3.7932 (-3) | 6.8527 (-3) | 1.15716 (-2) | 2.81516 ( |
| 90 | 2.4072 (-3) | 4.6664 (-3) | 8.3431 (-3) | 1.39583 (-2) | 3.34377 ( |
| 100 | 2.9189 (-3) | 5.6012 (-3) | 9.9233 (-3) | 1.64681 (-2) | 3.89256 ( |
| 110 | 3.4669 (-3) | 6.5927 (-3) | 1.15852 (-2) | 1.90890 (-2) | 4.45932 ( |
| 120 | 4.0499 (-3) | 7.6364 (-3) | 1.33220 (-2) | 2.18109 (-2) | 5.04222 ( |
| 130 | 4.6627 (-3) | 8.7287 (-3) | 1.51277 (-2) | 2.46253 (-2) | 5.63973 ( |
| 140 | 5.3056 (-3) | 9.8663 (-3) | 1.69972 (-2) | 2.75244 (-2) | 6.25058 ( |
| 150 | 5.9788 (-3) | 1.1046 (-2) | 1.89261 (-2) | 3.05021 (-2) | 6.87366 ( |

Table II. (continued)

| θ \ T | .90 | 1.00 | 1.10 | 1.20 | 1.30 |
|---|---|---|---|---|---|
| 20 | 7.5301 (-3) | 1.60831 (-2) | 3.06599 (-2) | 5.35096 (-2) | 8.71106 ( |
| 30 | 1.41960 (-2) | 2.88684 (-2) | 5.28479 (-2) | 8.92163 (-2) | 1.41328 ( |
| 40 | 2.18513 (-2) | 4.30695 (-2) | 7.68762 (-2) | 1.27150 (-1) | 1.98096 ( |
| 50 | 3.02361 (-2) | 5.82858 (-2) | 1.02203 (-1) | 1.66643 (-1) | 2.56648 ( |
| 60 | 3.91918 (-2) | 7.42830 (-2) | 1.28518 (-1) | 2.07319 (-1) | 3.16553 ( |
| 70 | 4.86127 (-2) | 9.09087 (-2) | 1.55623 (-1) | 2.48936 (-1) | 3.77536 ( |
| 80 | 5.84236 (-2) | 1.08056 (-1) | 1.83381 (-1) | 2.91330 (-1) | 4.39407 ( |
| 90 | 6.85684 (-2) | 1.25647 (-1) | 2.11691 (-1) | 3.34381 (-1) | 5.02027 ( |
| 100 | 7.90041 (-2) | 1.43622 (-1) | 2.40479 (-1) | 3.77997 (-1) | 5.65289 ( |
| 110 | 8.96964 (-2) | 1.61935 (-1) | 2.69685 (-1) | 4.22108 (-1) | 6.29103 ( |
| 120 | 1.00617 (-1) | 1.80547 (-1) | 2.99260 (-1) | 4.66657 (-1) | 6.93391 ( |
| 130 | 1.11745 (-1) | 1.99428 (-1) | 3.29168 (-1) | 5.11597 (-1) | 7.58078 ( |
| 140 | 1.23059 (-1) | 2.18552 (-1) | 3.59375 (-1) | 5.56886 (-1) | 8.23090 ( |
| 150 | 1.34544 (-1) | 2.37897 (-1) | 3.89854 (-1) | 6.02489 (-1) | 8.88354 ( |

Table III. A tabulation of $g_M$

| $\theta$ \ $\tau$ | .30 | .35 | .40 | .45 | .50 |
|---|---|---|---|---|---|
| 20 | 6.894 (-8) | 3.2322 (-7) | 1.2095 (-6) | 3.812 (-6) | 1.0392 ( |
| 30 | 1.8573(-7) | 8.531 (-7) | 3.123 (-6) | 9.531 (-6) | 2.5026 ( |
| 40 | 3.7304(-7) | 1.6852 (-6) | 6.033 (-6) | 1.7913 (-5) | 4.5609 ( |
| 50 | 6.381 (-7) | 2.8374 (-6) | 9.953 (-6) | 2.8855 (-5) | 7.1572 ( |
| 60 | 9.859 (-7) | 4.3197 (-6) | 1.4876 (-5) | 4.2222 (-5) | 1.02385( |
| 70 | 1.4204(-6) | 6.140 (-6) | 2.0779 (-5) | 5.7859 (-5) | 1.37574( |
| 80 | 1.9445(-6) | 8.295 (-6) | 2.7634 (-5) | 7.5624 (-5) | 1.7674 ( |
| 90 | 2.5602(-6) | 1.0787 (-5) | 3.5413 (-5) | 9.5381 (-5) | 2.1957 ( |
| 100 | 3.270 (-6) | 1.3612 (-5) | 4.4074 (-5) | 1.17003(-4) | 2.6517 ( |
| 110 | 4.073 (-6) | 1.6766 (-5) | 5.3587 (-5) | 1.40377(-4) | 3.1396 ( |
| 120 | 4.972 (-6) | 2.0244 (-5) | 6.3921 (-5) | 1.65402(-4) | 3.6542 ( |
| 130 | 5.966 (-6) | 2.4041 (-5) | 7.5041 (-5) | 1.9199 (-4) | 4.1932 ( |
| 140 | 7.055 (-6) | 2.8150 (-5) | 8.6918 (-5) | 2.2006 (-4) | 4.7547 ( |
| 150 | 8.240 (-6) | 3.2566 (-5) | 9.9521 (-5) | 2.4954 (-4) | 5.3368 ( |


APPROVED FOR PUBLIC RELEASE

Table III. (continued)

| θ \ τ | .55 | .60 | .65 | .70 | .80 |
|---|---|---|---|---|---|
| 20 | 2.5078 (-5) | 5.4482 (-5) | 1.08159 (-4) | 1.9861 (-4) | 5.5221 ( |
| 30 | 5.7922 (-5) | 1.2047 (-4) | 2.2925 (-4) | 4.0236 (-4) | 1.03250( |
| 40 | 1.02150 (-4) | 2.0578 (-4) | 3.7798 (-4) | 6.4465 (-4) | 1.56569 ( |
| 50 | 1.56114 (-4) | 3.0583 (-4) | 5.4849 (-4) | 9.1384 (-4) | 2.12982 ( |
| 60 | 2.1855 (-4) | 4.1848 (-4) | 7.3538 (-4) | 1.20241(-3) | 2.71274 ( |
| 70 | 2.8757 (-4) | 5.4130 (-4) | 9.3511 (-4) | 1.50539(-3) | 3.3071 ( |
| 80 | 3.6306 (-4) | 6.7260 (-4) | 1.14508 (-3) | 1.81925(-3) | 3.9081 ( |
| 90 | 4.4394 (-4) | 8.1102 (-4) | 1.36332 (-3) | 2.14141(-3) | 4.5126 ( |
| 100 | 5.2957 (-4) | 9.5550 (-4) | 1.58829 (-3) | 2.46993(-3) | 5.1184 ( |
| 110 | 6.1938 (-4) | 1.10520 (-3) | 1.81379 (-3) | 2.80336(-3) | 5.7240 ( |
| 120 | 7.1290 (-4) | 1.25931 (-3) | 2.05384 (-3) | 3.14053(-3) | 6.3283 ( |
| 130 | 8.0974 (-4) | 1.41726 (-3) | 2.29266 (-3) | 3.4806 (-3) | 6.9304 ( |
| 140 | 9.0954 (-4) | 1.57855 (-3) | 2.53461 (-3) | 3.8227 (-3) | 7.5297 ( |
| 150 | 1.01200 (-3) | 1.74275 (-3) | 2.77915 (-3) | 4.1664 (-3) | 8.1260 ( |

Table III. (continued)

| θ \ τ | .90 | 1.00 | 1.10 | 1.20 | 1.30 |
|---|---|---|---|---|---|
| 20 | 1.25428 (-3) | 2.44759 (-3) | 4.2568 (-3) | 6.7768 (-3) | 1.00706 |
| 30 | 2.18755 (-3) | 4.0252 (-3) | 6.6656 (-3) | 1.01877 (-2) | 1.46335 |
| 40 | 3.16732 (-3) | 5.6100 (-3) | 9.0035 (-3) | 1.34103 (-2) | 1.88551 |
| 50 | 4.1651 (-3) | 7.1766 (-3) | 1.13621(-2) | 1.64686 (-2) | 2.28061 |
| 60 | 5.1671 (-3) | 8.7158 (-3) | 1.34441(-2) | 1.93850 (-2) | 2.65357 |
| 70 | 6.1661 (-3) | 1.02245(-2) | 1.55549(-2) | 2.21760 (-2) | 3.00795 |
| 80 | 7.1580 (-3) | 1.17019(-2) | 1.76005(-2) | 2.48627 (-2) | 3.34642 |
| 90 | 8.1406 (-3) | 1.31487(-2) | 1.95861(-2) | 2.74512 (-2) | 3.67104 |
| 100 | 9.1126 (-3) | 1.45659(-2) | 2.15168(-2) | 2.99536 (-2) | 3.98344 |
| 110 | 1.00733 (-2) | 1.59549(-2) | 2.33969(-2) | 3.23783 (-2) | 4.28494 |
| 120 | 1.10224 (-2) | 1.73170(-2) | 2.52301(-2) | 3.47323 (-2) | 4.57662 |
| 130 | 1.19599 (-2) | 1.86535(-2) | 2.70200(-2) | 3.70217 (-2) | 4.85935 |
| 140 | 1.28858 (-2) | 1.99658(-2) | 2.87695(-2) | 3.92517 (-2) | 5.13386 |
| 150 | 1.38003 (-2) | 2.12549(-2) | 3.04813(-2) | 4.14267 (-2) | 5.40078 |


APPROVED FOR PUBLIC RELEASE

Table IV. The compressibility factor pv/NkT

| $\theta$ \ $T$ | .30 | .35 | .40 | .45 | .50 |
|---|---|---|---|---|---|
| 20 | 140.759 | 76.064 | 45.323 | 29.329 | 20.387 |
| 30 | 96.145 | 52.977 | 32.423 | 21.6791 | 15.625 |
| 40 | 73.819 | 41.400 | 25.925 | 17.7938 | 13.172 |
| 50 | 60.411 | 34.431 | 21.9935 | 15.4224 | 11.655 |
| 60 | 51.459 | 29.766 | 19.3490 | 13.8142 | 10.612 |
| 70 | 45.056 | 26.4227 | 17.4419 | 12.6433 | 9.845 |
| 80 | 40.248 | 23.9022 | 15.9972 | 11.7491 | 9.253 |
| 90 | 36.498 | 21.9324 | 14.8630 | 11.0408 | 8.780 |
| 100 | 33.495 | 20.3487 | 13.9455 | 10.4641 | 8.389 |
| 110 | 31.032 | 19.0462 | 13.1866 | 9.9838 | 8.061 |
| 120 | 28.976 | 17.9551 | 12.5475 | 9.5767 | 7.782 |
| 130 | 27.231 | 17.0267 | 12.0011 | 9.2265 | 7.539 |
| 140 | 25.733 | 16.2266 | 11.5377 | 8.9214 | 7.326 |
| 150 | 24.431 | 15.5291 | 11.1131 | 8.6528 | 7.137 |


APPROVED FOR PUBLIC RELEASE

Table IV. (continued)

| θ \ τ | .55 | .60 | .65 | .70 | .80 |
|---|---|---|---|---|---|
| 20 | 15.084 | 11.7672 | 9.5937 | 8.1066 | 6.265 |
| 30 | 11.9874 | 9.6722 | 8.1260 | 7.0330 | 5.635 |
| 40 | 10.3598 | 8.5444 | 7.3015 | 6.4150 | 5.247 |
| 50 | 9.3357 | 7.8145 | 6.7618 | 5.9987 | 4.974 |
| 60 | 8.6224 | 7.2977 | 6.3715 | 5.6921 | 4.766 |
| 70 | 8.0861 | 6.9066 | 6.0717 | 5.4535 | 4.601 |
| 80 | 7.6689 | 6.5971 | 5.8317 | 5.2605 | 4.466 |
| 90 | 7.3315 | 6.3442 | 5.6337 | 5.0997 | 4.351 |
| 100 | 7.0516 | 6.1324 | 5.4664 | 4.9630 | 4.253 |
| 110 | 6.8144 | 5.9516 | 5.3224 | 4.8447 | 4.166 |
| 120 | 6.6102 | 5.7945 | 5.1968 | 4.7408 | 4.090 |
| 130 | 6.4318 | 5.6566 | 5.0858 | 4.6486 | 4.022 |
| 140 | 6.2742 | 5.5340 | 4.9867 | 4.5660 | 3.961 |
| 150 | 6.1337 | 5.4241 | 4.8974 | 4.4913 | 3.905 |

Table IV. (continued)

| θ \ T | .90 | 1.00 | 1.10 | 1.20 | 1.30 |
|---|---|---|---|---|---|
| 20 | 5.2018 | 4.51787 | 4.04135 | 3.69940 | 3.418 |
| 30 | 4.7837 | 4.22220 | 3.81596 | 3.50972 | 3.270 |
| 40 | 4.5176 | 4.01831 | 3.65450 | 3.37715 | 3.158 |
| 50 | 4.3200 | 3.86584 | 3.53141 | 3.27457 | 3.071 |
| 60 | 4.16681 | 3.74554 | 3.43320 | 3.19198 | 3.000 |
| 70 | 4.04293 | 3.64755 | 3.35424 | 3.12344 | 2.940 |
| 80 | 3.93975 | 3.56479 | 3.28376 | 3.06522 | 2.890 |
| 90 | 3.85187 | 3.49399 | 3.22479 | 3.01486 | 2.846 |
| 100 | 3.77568 | 3.43229 | 3.17319 | 2.97065 | 2.807 |
| 110 | 3.70871 | 3.37781 | 3.12746 | 2.93137 | 2.773 |
| 120 | 3.64915 | 3.32918 | 3.08652 | 2.89613 | 2.742 |
| 130 | 3.59508 | 3.28537 | 3.04955 | 2.86423 | 2.714 |
| 140 | 3.54727 | 3.24559 | 3.01592 | 2.83513 | 2.688 |
| 150 | 3.50314 | 3.20924 | 2.98512 | 2.80843 | 2.664 |

Table V. The reduced internal energy of gas imperfection $E'/N\epsilon^*$

| $\theta$ \ $T$ | .30 | .35 | .40 | .45 | .50 |
|---|---|---|---|---|---|
| 20 | 617.84 | 315.44 | 175.30 | 104.53 | 66.328 |
| 30 | 632.32 | 329.52 | 188.84 | 117.37 | 78.390 |
| 40 | 646.61 | 343.30 | 201.21 | 129.65 | 89.811 |
| 50 | 660.75 | 356.79 | 213.47 | 141.47 | 100.705 |
| 60 | 674.70 | 370.02 | 225.60 | 152.91 | 111.177 |
| 70 | 688.50 | 383.06 | 237.68 | 164.00 | 121.294 |
| 80 | 702.15 | 395.86 | 249.57 | 174.78 | 131.112 |
| 90 | 715.65 | 408.45 | 261.48 | 185.30 | 140.673 |
| 100 | 729.07 | 420.86 | 273.32 | 195.58 | 149.93 |
| 110 | 742.30 | 433.09 | 284.95 | 205.65 | 159.01 |
| 120 | 755.41 | 445.00 | 295.90 | 215.53 | 167.90 |
| 130 | 768.40 | 457.06 | 307.66 | 225.23 | 176.61 |
| 140 | 781.28 | 468.82 | 317.27 | 234.78 | 185.17 |
| 150 | 794.05 | 480.44 | 327.72 | 244.17 | 193.58 |


APPROVED FOR PUBLIC RELEASE

Table V. (continued)

| θ \ τ | .55 | .60 | .65 | .70 | .80 |
|---|---|---|---|---|---|
| 20 | 44.554 | 31.55 | 23.398 | 18.112 | 12.01 |
| 30 | 55.793 | 41.947 | 33.057 | 27.004 | 19.66 |
| 40 | 66.323 | 51.665 | 41.943 | 35.219 | 26.70 |
| 50 | 76.333 | 60.803 | 50.347 | 42.955 | 33.33 |
| 60 | 85.928 | 69.543 | 58.355 | 50.321 | 39.65 |
| 70 | 95.104 | 77.942 | 66.045 | 57.394 | 45.73 |
| 80 | 104.010 | 86.057 | 73.471 | 64.226 | 51.61 |
| 90 | 112.657 | 93.928 | 80.672 | 70.852 | 57.32 |
| 100 | 121.076 | 101.588 | 87.679 | 77.301 | 62.88 |
| 110 | 129.293 | 109.064 | 94.516 | 83.596 | 68.31 |
| 120 | 137.330 | 116.370 | 101.202 | 89.754 | 73.64 |
| 130 | 145.204 | 123.527 | 107.753 | 95.790 | 78.86 |
| 140 | 152.930 | 130.550 | 114.180 | 101.714 | 83.99 |
| 150 | 160.521 | 137.448 | 120.497 | 107.538 | 89.03 |


APPROVED FOR PUBLIC RELEASE

Table V. (continued)

| $\theta$ \ $\tau$ | .90 | 1.00 | 1.10 | 1.20 | 1. |
|---|---|---|---|---|---|
| 20 | 8.8603 | 6.9966 | 5.7941 | 4.9620 | 4.35 |
| 30 | 15.4864 | 12.8358 | 11.0137 | 9.6879 | 8.68 |
| 40 | 21.6171 | 18.2619 | 15.8873 | 14.1211 | 12.75 |
| 50 | 27.406 | 23.4027 | 20.5202 | 18.3486 | 16.65 |
| 60 | 32.939 | 28.3285 | 24.9709 | 22.4193 | 20.41 |
| 70 | 38.268 | 33.0836 | 29.2760 | 26.3644 | 24.06 |
| 80 | 43.431 | 37.6980 | 33.4610 | 30.2051 | 27.62 |
| 90 | 48.452 | 42.1935 | 37.5439 | 33.9570 | 31.10 |
| 100 | 53.352 | 46.5863 | 41.5387 | 37.6319 | 34.52 |
| 110 | 58.145 | 50.8891 | 45.4559 | 41.2389 | 37.87 |
| 120 | 62.845 | 55.1121 | 49.3041 | 44.7853 | 41.16 |
| 130 | 67.460 | 59.2635 | 53.0904 | 48.2770 | 44.40 |
| 140 | 72.000 | 63.3500 | 56.8205 | 51.7189 | 47.60 |
| 150 | 76.469 | 67.3775 | 60.4994 | 55.1147 | 50.74 |



APPROVED FOR PUBLIC RELEASE

Table VI. The reduced entropy of gas imperfection S'/Nk

| θ \ τ | .30 | .35 | .40 | .45 | .5 |
|---|---|---|---|---|---|
| 20 | 7.5145 | 6.6025 | 5.8279 | 5.1649 | 4.59 |
| 30 | 6.9274 | 6.0310 | 5.2785 | 4.6436 | 4.10 |
| 40 | 6.5161 | 5.6346 | 4.9018 | 4.2899 | 3.77 |
| 50 | 6.2005 | 5.3334 | 4.6181 | 4.0260 | 3.53 |
| 60 | 5.9461 | 5.0921 | 4.3924 | 3.8174 | 3.34 |
| 70 | 5.7335 | 4.8910 | 4.2062 | 3.6465 | 3.18 |
| 80 | 5.5512 | 4.7202 | 4.0485 | 3.5025 | 3.05 |
| 90 | 5.3922 | 4.5719 | 3.9121 | 3.3786 | 2.94 |
| 100 | 5.2509 | 4.4411 | 3.7926 | 3.2702 | 2.84 |
| 110 | 5.1248 | 4.3246 | 3.6865 | 3.1742 | 2.75 |
| 120 | 5.0107 | 4.2200 | 3.5912 | 3.0883 | 2.68 |
| 130 | 4.9068 | 4.1243 | 3.5050 | 3.0106 | 2.61 |
| 40 | 4.8113 | 4.0371 | 3.4264 | 2.9399 | 2.54 |
| 50 | 4.7232 | 3.9570 | 3.3543 | 2.8750 | 2.49 |


APPROVED FOR PUBLIC RELEASE

Table VI. (continued)

| $\theta$ \ $\tilde{T}$ | .55 | .60 | .65 | .70 | .80 |
|---|---|---|---|---|---|
| 20 | 4.1065 | 3.6352 | 3.3216 | 3.0069 | 2.4945 |
| 30 | 3.6498 | 3.2617 | 2.9289 | 2.6917 | 2.1942 |
| 40 | 3.3463 | 2.9817 | 2.67319 | 2.40846 | 1.9613 |
| 50 | 3.1229 | 2.7778 | 2.48549 | 2.23563 | 1.8132 |
| 60 | 2.9478 | 2.6184 | 2.33939 | 2.10129 | 1.7179 |
| 70 | 2.80653 | 2.48885 | 2.22079 | 1.99221 | 1.6241 |
| 80 | 2.68756 | 2.38046 | 2.1216 | 1.90096 | 1.5456 |
| 90 | 2.58569 | 2.28773 | 2.03676 | 1.82290 | 1.4783 |
| 100 | 2.49697 | 2.20701 | 1.96291 | 1.75493 | 1.4197 |
| 110 | 2.41863 | 2.13575 | 1.89774 | 1.69493 | 1.3679 |
| 120 | 2.34869 | 2.07216 | 1.83955 | 1.64134 | 1.3216 |
| 130 | 2.28566 | 2.01487 | 1.78711 | 1.59302 | 1.2798 |
| 140 | 2.22840 | 1.96283 | 1.73947 | 1.54911 | 1.2418 |
| 150 | 2.17602 | 1.91523 | 1.69589 | 1.50893 | 1.2069 |


APPROVED FOR PUBLIC RELEASE

Table VI. (continued)

| θ \ T | .90 | 1.00 | 1.10 | 1.20 | 1. |
|---|---|---|---|---|---|
| 20 | 2.09945 | 1.78771 | 1.53613 | 1.32891 | 1.155 |
| 30 | 1.82995 | 1.55025 | 1.32391 | 1.13660 | 0.979 |
| 40 | 1.65331 | 1.39392 | 1.18351 | 1.00910 | .861 |
| 50 | 1.52400 | 1.27911 | 1.08005 | 0.91469 | .774 |
| 60 | 1.42307 | 1.18925 | 0.99886 | .84044 | .706 |
| 70 | 1.34088 | 1.11592 | .93247 | .77970 | .649 |
| 80 | 1.27193 | 1.05488 | .87657 | .72830 | .602 |
| 90 | 1.21277 | 1.00132 | .82847 | .68410 | .561 |
| 100 | 1.16114 | 0.95503 | .78637 | .64537 | .525 |
| 110 | 1.11544 | .91401 | .74903 | .61099 | .493 |
| 120 | 1.07455 | .87726 | .71555 | .58013 | .464 |
| 130 | 1.03760 | .84403 | .68524 | .55218 | .438 |
| 140 | 1.00396 | .81374 | .65759 | .52667 | .415 |
| 150 | 0.97312 | .78596 | .63221 | .50324 | .393 |

Section 2.

## Calculation of Detonation Velocity with the Free Volume Equation of State.

The method of reference (1) has been somewhat modified and is briefly described in the following. The Hugoniot equation can be written in the reduced variables as

$$\frac{\bar{C}_v^{\circ}(T)}{R}\theta + \varepsilon' - \frac{Q}{N_A \bar{\varepsilon}^*} - \frac{1}{2}\mathcal{N}\theta\left(\tau_0/\tau - 1\right) \qquad (2\text{-}1)$$

where

$$Q = -\sum_i x_i \Delta H_{fi}^{\circ} + \frac{M}{M_0}\Delta H_{f_0} + H^{\circ}(T_0) \qquad (2\text{-}2)$$

$$\bar{C}_v^{\circ}(T) = \frac{E^{\circ}(T) - E^{\circ}(0)}{T} \qquad (2\text{-}3)$$

and

$$\tau_0 = \frac{M/\rho_0}{\bar{v}^*} \qquad (2\text{-}4)$$

We consider here only the case in which all of the products are gaseous. All extensive thermodynamic functions are taken for one mole of the gaseous mixture, or one mole of pure component i as appropriate. Here $x_i$ is the mole fraction of component i in the final state; $\Delta H_{fi}^{\circ}$ is the standard molar enthalpy of formation of component i at $T_o$, $\Delta H_{fo}^{\circ}$ that of the explosive; $M_o$ is the molecular weight of the explosive, and M is the mass of explosive producing one mole of product gas. $H^{\circ}(T)$ and $E^{\circ}(T)$ denote the molar enthalpy and internal energy of the product gas (with composition fixed at the $x_i$) at infinite volume at temperature T. The initial explosive density is denoted by $\rho_0$. The reduced variables $\tau$, $\theta$, $\mathcal{N}$, and $\varepsilon'$ are defined as Section 1, except that v* and $\epsilon$* are replaced by $\bar{v}$* and $\bar{\varepsilon}$* as in reference (1).



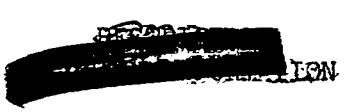

The detonation velocity $\mathcal{D}$ corresponding to this transition is given by

$$\mathcal{D}^2 = \frac{N_A \bar{\epsilon}^*}{M} \frac{T_0^2}{T^2} \frac{2\theta}{\frac{T_0}{T} - 1} \qquad (2\text{-}5)$$

The Chapman-Jouget condition may be stated as

$$D = \min \mathcal{D} \text{ with } T_0/T > 1 \qquad (2\text{-}6)$$

D being the actual steady detonation velocity achieved.

We note that $\bar{v}^*$ does not appear explicitly in (1) and (5). Thus for a given explosive and an assumed fixed composition in the final state (the equations for chemical equilibrium cannot be written in reduced form without explicit appearance of $\bar{v}^*$ except in special cases) D can be found as a function of two independent variables $T_0$ and $N_A\bar{\epsilon}^*$. Comparison with experiment cannot be made without relating $T_0$ to $\rho_0$ by (4), which contains $\bar{v}^*$, but this transformation is easily made, and it is a considerable simplification that (1), (5), and (6) do not have to be solved for each different $\bar{v}^*$.

The present numerical procedure is as follows. For a given and $N_A\bar{\epsilon}^*$, three or four equally spaced values of $T$ known from experience to bracket the C-J value are selected. The required interval in $T$ is smaller than the tabular interval, so that the interpolation procedures mentioned in the preceding section are used in obtaining corresponding values of the dependent variables. Equation (2-1) is then solved for $\theta$ at each of these values of $T$. To do this it has been found satisfactory to evaluate the left hand side of (2-1) for the three tabular values of $\theta$ closest to the solution, then finding by three point Lagrangian interpolation the value of $\theta$ which



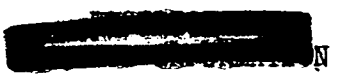

have a section of the Hugoniot curve, with values of $T$, $\mathcal{H}$, and $\mathcal{D}$ (from (2-5)) known for each $T$. The minimum $\mathcal{D} = D$ and the corresponding values of $T$, $\mathcal{H}$, etc. are then found by Lagrangian interpolation.

No calculations have been made to date for other than fixed composition. The procedure when chemical equilibrium is assumed will be appreciably more complicated. The procedure presently used requires about 2-1/2 hours per pair of values of $T_0$ and $N\bar{c}*$ when a desk calculator is used. The method has been adapted to the IBM CPEC Model II combination; on this, exclusive of set-up time, about 15 minutes are required.



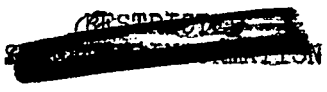

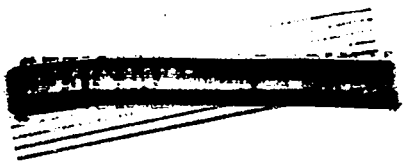

## Calculations for RDX

At present calculations have been made for only one explosive, RDX, $(CH_2NNO_2)_3$, cyclotrimethylenetrinitramine. This explosive was chosen on the recommendation of E. H. Eyster because it is the member of the family of explosives having composition balanced to CO, $H_2O$, and $N_2$ for which the most extensive experimental detonation velocity measurements have been made. The balanced composition was considered desirable because it was felt that it would permit greater certainty about the composition than in other cases.

In our calculations we have used the values of the physical constants and the ideal gas values of the thermodynamic functions of the various component gases as tabulated by the National Bureau of Standards.[4] We have assumed the decomposition to be to CO, $H_2O$, and $N_2$; corresponding to this process we used $Q = 31.482 \frac{\text{Kcal}}{\text{mole gas}}$, using a value for the internal energy of combustion of -501.82 Kcal/mole RDX.[5] We have taken $T_o$ as 25°C.

As discussed in reference (1), and as will be seen later in this report, there are many reasons for suspecting that the Lennard-Jones (6,12) intermolecular potential may not adequately represent the actual situation in the region of internuclear distances attained in detonation, particularly if the same constants $N_A\epsilon^*$ and $v^*$ as found from the usual low temperature

---

[4] N.B.S. "Selected Values of Chemical Thermodynamic Properties."

[5] We have lately learned (private communication, D.V.Sickman to L.C.Smith) that this figure is actually the National Bureau of Standards $\Delta H$ of combustion. This gives $Q = 31.877$ Kcal/mole.




viscosity and virial coefficient date are used. (These latter lead to the values $N_A\bar{\epsilon}^* = 224 \frac{cal}{mole}$, $\bar{v}^* = 25.48 \frac{cm^3}{mole}$). Thus we are led to first inquire as to whether values of $N_A\bar{\epsilon}^*$ and $\bar{v}^*$ can be found such that the calculated detonation velocities adequately represent those obtained experimentally throughout the loading density range. Under our assumption of fixed composition this can be done without regard to the question of assigning individual values to the $N_A\epsilon_i^*$ and $v_i^*$.

As mentioned in Section 2 it is most convenient to compute D as a function of $\tau_o$ and $N_A\bar{\epsilon}^*$. The results are shown in Table 7. Our present comparison with experiment is based on the interpretation of the RDX data in OSRD 5611 in terms of a linear relation between the infinite-diameter rate and the loading density $\rho_o^6$. Work is underway in GMX-2 and GMX-8 to determine the validity of this assumption, particularly in the high density range. For the present, however, we use

$$D_{exp} = 2597 + 3540 \rho_o \quad m/sec. \quad (\rho_o \text{ in } g/cm^3) \qquad (3\text{-}1)$$

The standard deviation of the experimental points from (3-1) is estimated to be about 50 m/sec. However, the only experimental points for densities greater than 1.52 $g/m^3$ are the three small charges of very high density (1.77 $g/m^3$) obtained by GMX-2 and GMX-8. When corrected for diameter effect according to reference (5b), they fall about 170 m/sec. below Equation (3-1). The high density region is accordingly poorly defined experimentally.

Equation (3-1) may be written, by use of (2-4) in the form

$$D_{exp} = 2597 + 3540 \frac{M}{\bar{v}^*} \tau_o^{-1} \qquad (3\text{-}2)$$

---

[6](a) OSRD 5611; (b) GMX-2 memorandum from W. W. Wood to L. C. Smith dated September 4, 1951.



TABLE 7

| $N_A \bar{\epsilon}^*$ cal / mole gas | $\tau_0$ | $\tau_0^{-1}$ | $\tau$ | $\tau^{-1}$ | $\tau/\tau_0$ | $\theta$ | $D$ m/sec | $T$ °K | $P\bar{v}^*$ megabars x cm³/mole gas |
|---|---|---|---|---|---|---|---|---|---|
| 60 | 0.4500 | 2.222 | 0.3643 | 2.745 | 0.810 | 103.6 | 10981 | 3128 | 12.6 |
| | .5500 | 1.818 | .4330 | 2.309 | .787 | 124.2 | 8787 | 3751 | 7.37 |
| | .7100 | 1.408 | .5385 | 1.857 | .758 | 137.4 | 7054 | 4148 | 4.179 |
| | 1.0000 | 1.000 | .7238 | 1.382 | .724 | 145.7 | 5684 | 4400 | 2.203 |
| | 1.5000 | 0.6667 | 1.0365 | 0.965 | .691 | 150.1 | 4724 | 4532 | 1.134 |
| 100 | 0.5000 | 2.000 | 0.4060 | 2.463 | 0.812 | 63.5 | 11205 | 3196 | 11.7 |
| | .6250 | 1.600 | .4920 | 2.033 | .787 | 76.9 | 8713 | 3870 | 6.38 |
| | .8250 | 1.212 | .6239 | 1.603 | .756 | 84.5 | 6881 | 4251 | 3.453 |
| | 1.1500 | 0.8696 | .8308 | 1.204 | .722 | 88.6 | 5604 | 4461 | 1.871 |
| | 1.4750 | .6780 | 1.0350 | 0.966 | .702 | 90.2 | 4976 | 4538 | 1.236 |
| | 1.8000 | .5556 | 1.2357 | .809 | .686 | 91.0 | 4595 | 4579 | 0.9079 |
| 200 | 0.5000 | 2.000 | 0.4143 | 0.214 | 0.829 | 25.2 | 14062 | 2535 | 16.7 |
| | .6000 | 1.667 | .4870 | 2.053 | .812 | 35.1 | 10920 | 3536 | 9.24 |
| | .7500 | 1.333 | .5897 | 1.696 | .786 | 40.8 | 8503 | 4104 | 3.815 |
| | .9300 | 1.075 | .7081 | 1.412 | .761 | 43.4 | 7052 | 4364 | 3.145 |
| | 1.6000 | 0.625 | 1.1315 | 0.884 | .707 | 45.8 | 5114 | 4606 | 1.185 |
| 300 | 0.625 | 1.600 | 0.5111 | 1.957 | 0.818 | 23.5 | 11692 | 3541 | 9.84 |
| | .74071 | 1.350 | .5922 | 1.689 | .800 | 27.0 | 9470 | 4069 | 5.90 |
| | .90901 | 1.100 | .7048 | 1.419 | .775 | 29.0 | 7715 | 4385 | 3.63 |
| | 1.17647 | 0.8500 | .8776 | 1.139 | .746 | 30.3 | 6333 | 4568 | 2.137 |
| | 1.66667 | .6000 | 1.1879 | 0.842 | .713 | 30.9 | 5204 | 4663 | 1.152 |

...us when $D_{exp}$ is plotted against $\tau_o^{-1}$, we obtain a family of centered straight lines whose slope depends on the value assigned to the theoretical parameter $\bar{v}^*$. Accordingly, a plot of the calculated D and $D_{exp}$ vs $\tau_o^{-1}$ on the same axes affords the desired comparison. Agreement would consist in acceptable coincidence of two curves, one from each family. Such a plot is shown in Figure 1. For convenience the density corresponding experimentally to a given detonation velocity is indicated on the right hand side of the figure. The solid horizontal lines indicate the extremes of the experimental region; the dashed ones the limits of the presently well defined experimental region as suggested by D. P. MacDougall. Figures 2 and 3 show respectively the dependence of the calculated C-J temperature and reduced density on $\tau_o^{-1}$.

For each of the four values of $N_A\bar{\epsilon}^*$ we have chosen $\bar{v}^*$ so as to minimize

$$\sigma^2 = \frac{\int_{1.0}^{1.6} (D-D_{exp})^2 d\rho_o}{\int_{1.0}^{1.6} d\rho_o}$$

These values of $\bar{v}^*$ and the corresponding values of $\sigma$, as well as the resulting values of D, $\rho$, $p$ and T as functions of $\rho_o$ are shown in Table 8. These numbers were read off graphs constructed from Table 7, and are not as accurate as the latter. The value of $\sigma$ is seen to decrease with decrease in $N_A\bar{\epsilon}^*$, while $\bar{v}^*$ increases. The range of Tables 1 to 6 does not permit calculation for $N_A\bar{\epsilon}^* < 60 \frac{cal}{mole}$ at present. It may be suspected that $\bar{v}^*$ will approach $\infty$ as $N_A\bar{\epsilon}^*$ approaches zero; the behavior of $\sigma$ is harder to predict. It seems unlikely that $\sigma$ will decrease below 100 m/sec., but detailed calculations would be required to prove this.

Figure 4 is a graph of $D - D_{exp}$ vs $\rho_o$ for these optimum pairs (the $N_A\bar{\epsilon}^* = 200$ curve falls between those for 100 and 300; it is not shown in the figure to avoid confusion). From this figure it seems unlikely that substantial

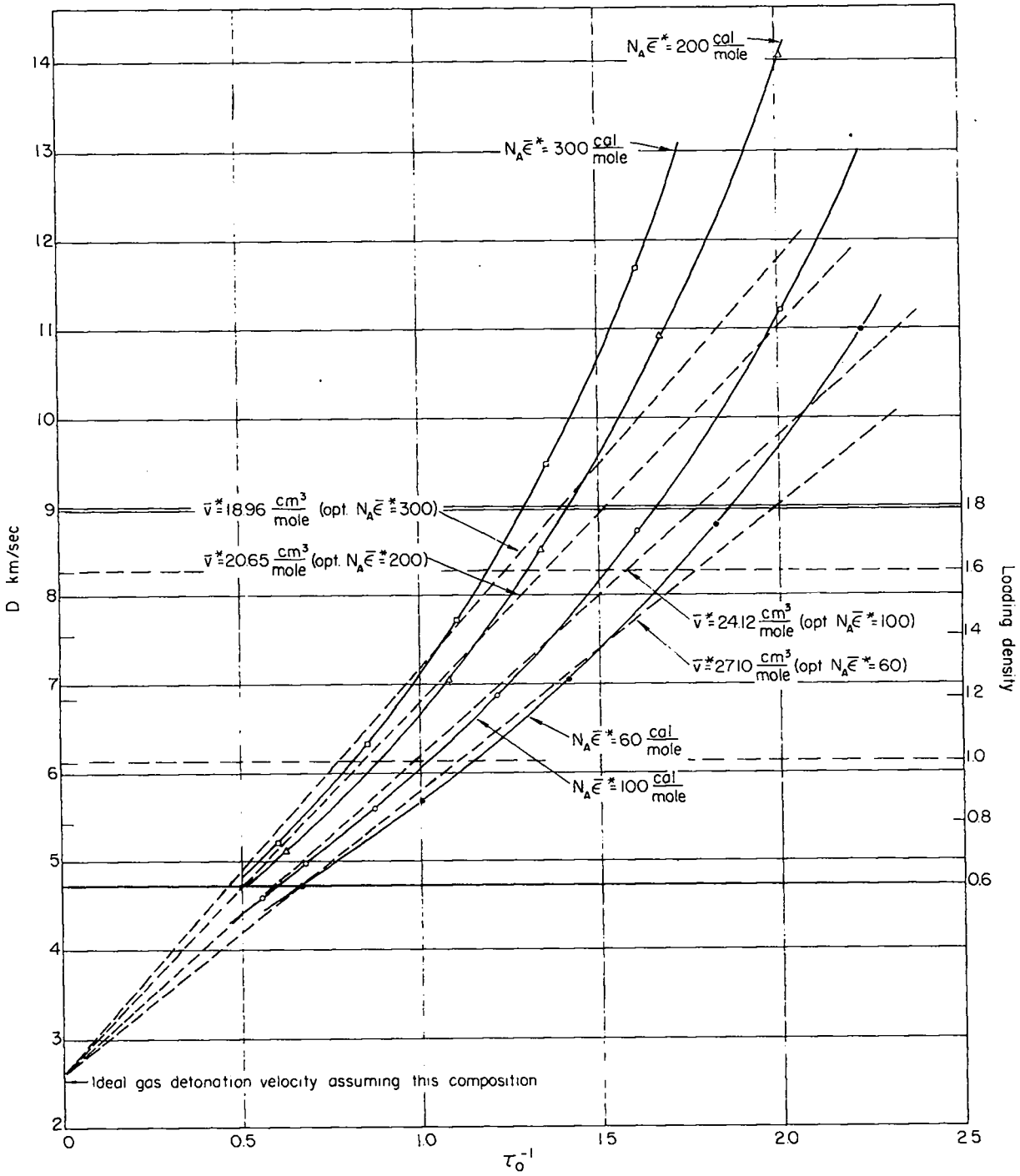


Figure 1. Detonation velocity vs. reduced loading density. Solid curves theoretical, dashed curves experimental.

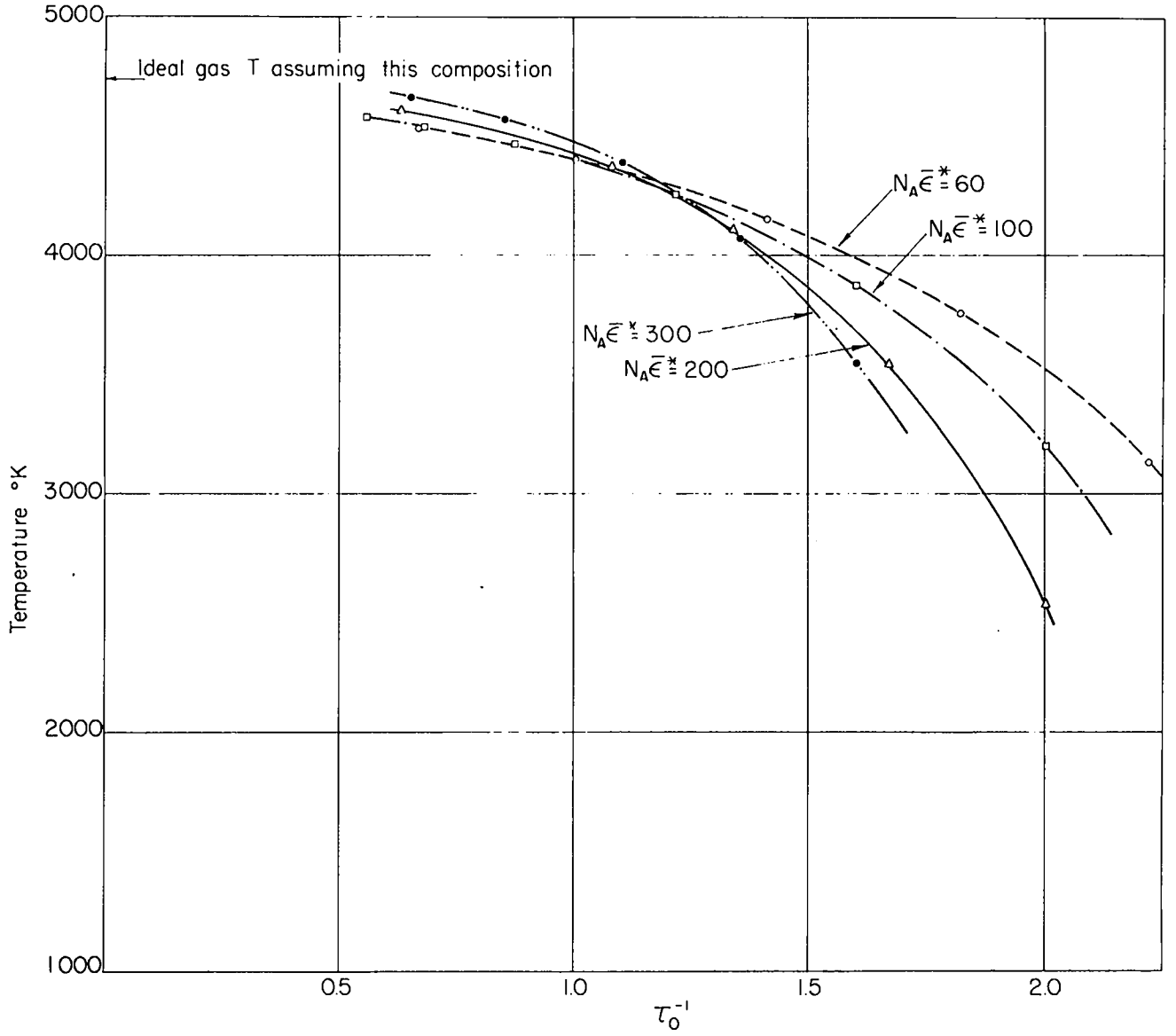


Figure 2. Chapman-Jouget temperature vs. reduced loading density.

APPROVED FOR PUBLIC RELEASE

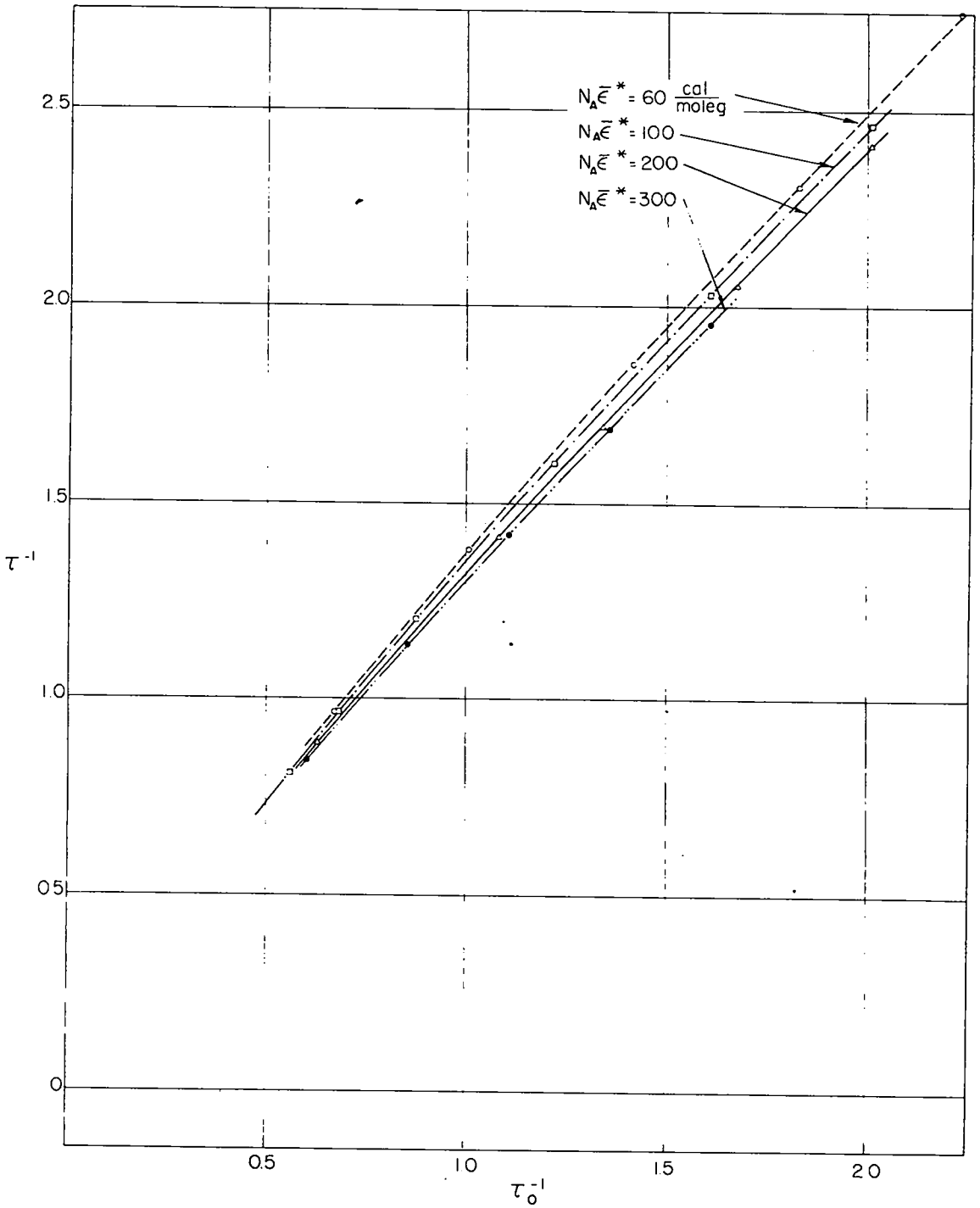


Figure 3. Chapman-Jouget reduced density vs. initial reduced density.

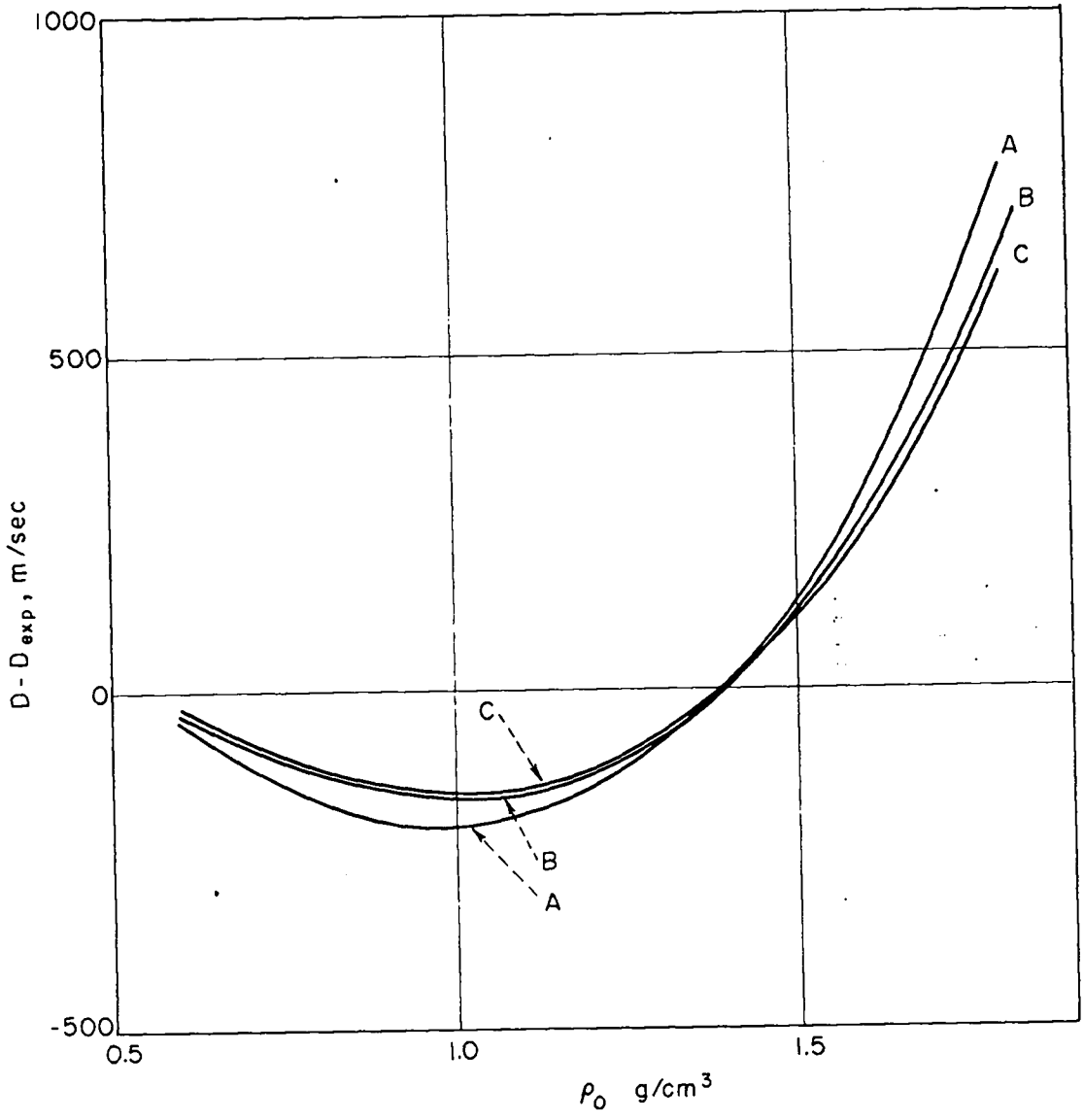


Figure 4. Deviation plot, detonation velocity vs. loading density. A, $N_A\bar{\epsilon}^* = 300 \frac{cal}{mole}$, $\bar{v}^* = 18.96 \frac{cm^3}{mole}$; B, 100 and 24.12; C, 60 and 27.10, respectively.

TABLE 8

| $\bar{N}_A$ * cal/mole | $\bar{v}$* cm³/mole | $\sigma$ m/sec | | $\rho_0$ g/cm³ | | | | | | |
|---|---|---|---|---|---|---|---|---|---|---|
| | | | | 0.6 | 0.8 | 1.0 | 1.2 | 1.4 | 1.6 | 1.8 |
| 60 | 27.10 | 118 | D, m/sec | 4700 | 5315 | 5990 | 6730 | 7555 | 8500 | 9590 |
| | | | ρ, g/cm³ | 0.870 | 1.124 | 1.366 | 1.599 | 1.824 | 2.044 | 2.262 |
| | | | P, m b. | 0.0411 | 0.0651 | .096 | 0.136 | 0.186 | 0.251 | 0.338 |
| | | | T, °K. | 4538 | 4452 | 4352 | 4217 | 4040 | 3822 | 3543 |
| 100 | 24.12 | 125 | D | 4685 | 5310 | 5980 | 6725 | 7555 | 8520 | 9620 |
| | | | ρ | 0.867 | 1.120 | 1.365 | 1.595 | 1.820 | 2.040 | 2.255 |
| | | | P | 0.0406 | 0.0644 | .096 | 0.134 | 0.184 | 0.251 | 0.336 |
| | | | T | 4570 | 4505 | 4407 | 4281 | 4123 | 3916 | 3638 |
| 200 | 20.65 | 143 | D | 4685 | 5280 | 5945 | 6705 | 7565 | 8545 | 9680 |
| | | | ρ | 0.868 | 1.118 | 1.359 | 1.590 | 1.814 | 2.033 | 2.247 |
| | | | P | 0.0407 | 0.0634 | 0.093 | 0.132 | 0.183 | 0.249 | 0.336 |
| | | | T | 4646 | 4590 | 4517 | 4416 | 4282 | 4095 | 3845 |
| 300 | 18.96 | 151 | D | | 5270 | 5940 | 6705 | 7575 | 8560 | 9740 |
| | | | ρ | | 1.119 | 1.359 | 1.588 | 1.812 | 2.029 | 2.245 |
| | | | P | | 0.0633 | 0.093 | 0.132 | 0.183 | 0.248 | 0.338 |
| | | | T | | 4661 | 4606 | 4527 | 4400 | 4243 | 4015 |
| Experimental D from equation (3-1) | | | | 4721 | 5429 | 6137 | 6845 | 7553 | 8261 | 8969 |



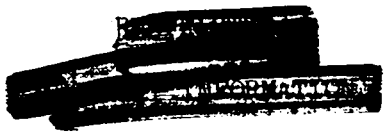

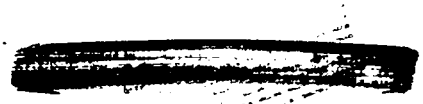

improvement would be obtained with smaller $N_A\bar{\epsilon}^*$. The uncertainity of the experimental data makes difficult a definite decision as to how well the present calculations agree with experiment. We are inclined to believe that the apparent disagreement is genuine, but have postponed a definite decision pending completion of the current experimental investigation, since it is clear that the high density region is of particular interest in this connection.

It is of interest to note that the pair of values $N_A\bar{\epsilon}^* = 224 \frac{cal}{mole}$, $\bar{v}^* = 25.48 \frac{cm^3}{mole}$ calculated from the L-J potential parameters obtained from low temperature virial coefficients lead to extreme disagreement in detonation velocity throughout the loading density region. The significance of this is obscured by the uncertainity in the intermolecular potential of water, as discussed in reference (1). However, not all the blame can be put on water, at least not if we continue to assume a L-J potential for it. This is evident from the fact that if one takes for $N_2$ and CO their second virial coefficient values ($\frac{\epsilon^*}{k} = 95.2° k.$, $v^* = 29.9 \frac{cm^3}{mole}$ will suffice for both) and for the averages $\bar{\epsilon}^*$ and $\bar{v}^*$ takes in succession the four best pairs of values, and then attempts to solve for the water parameters, one finds that there is no solution in any of the four cases. Evidently if our present assumptions are valid at all, the potential parameters for $N_2$ and CO will require appreciable modification.



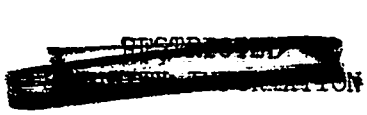

Section 4.

## Expected Development of the Investigation

As mentioned in Section 3, an experimental program is under way in GMX-2 and GMX-8 to obtain precise detonation velocity data for RDX, especially in the high density region. It is believed that these results will be available in the near future. If, as we expect, the apparent divergence of calculation and experiment in the high density region is proved to be real, we must then seek the explanation. The results of the trinitrotriazidobenzene and hexanitrosobenzene experimental programs mentioned in reference (1) will of course be of considerable help in this connection, when obtained. Certain improvements in the theory suggest themselves, and are discussed below.

It is of intrinsic interest to examine the predictions of this equation of state under the assumption of chemical equilibrium at the C-J plane, instead of assuming a fixed composition. The appropriate equations will be given in the revision of reference (1) mentioned in the introduction. In taking this step we are of course confronted with the already mentioned difficulty of the uncertainty of the relevant Lennard-Jones potential parameters for some components such as $H_2O$, in particular, and possibly, in the region of intermolecular distances of interest, even for such components as CO and $N_2$. It is of course an open question whether the use of a spherically symmetric potential for $H_2O$ and $CO_2$ will give a reasonable approximation. Furthermore, solid carbon is a possible component, and calculations with it present will require its equation of state. Estimates of the latter have been made in T division, and can be used here. At present we have made



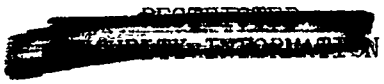

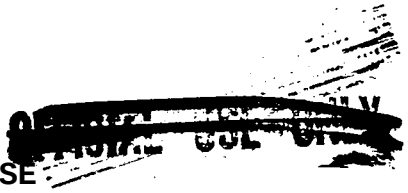

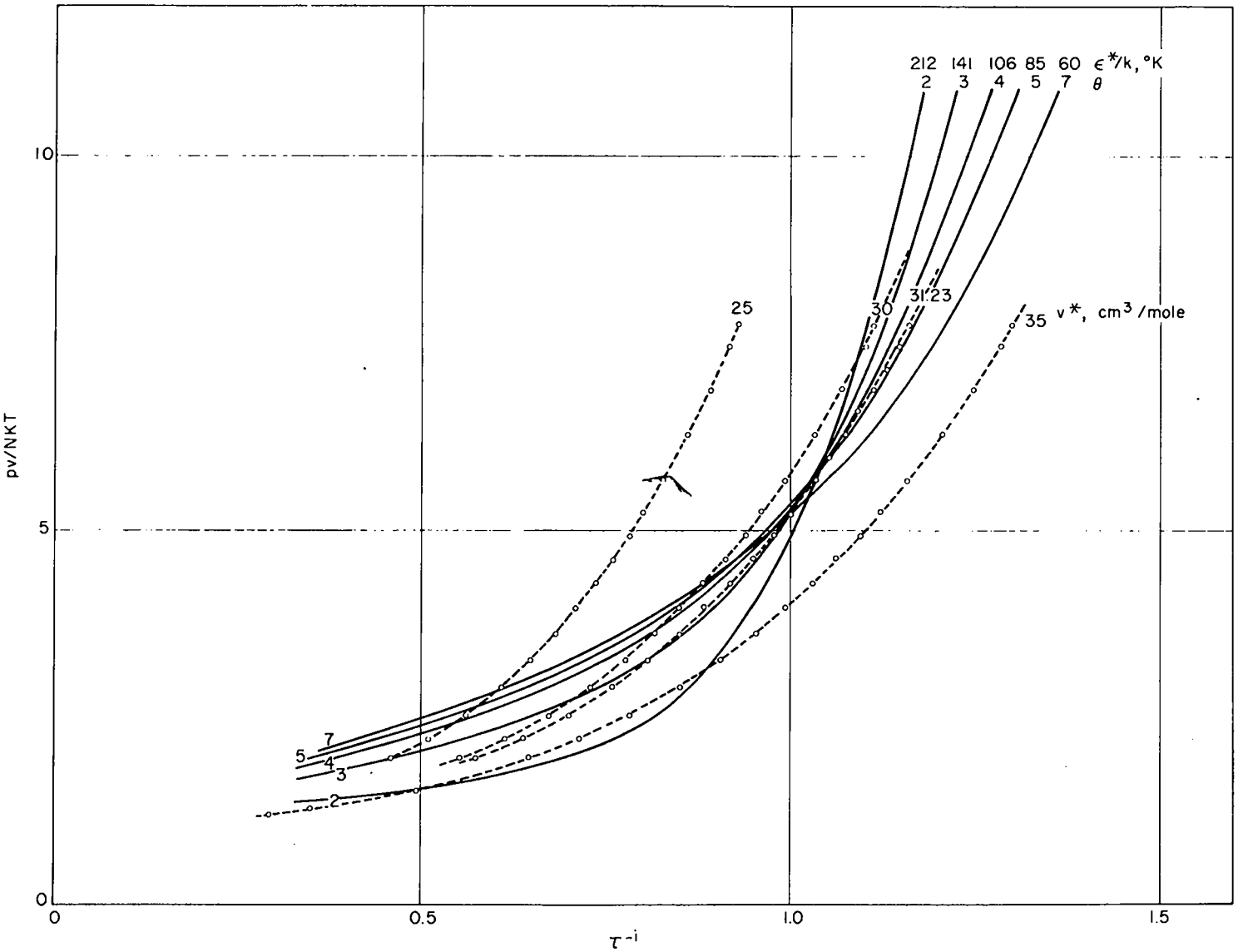


Figure 5. Theoretical and experimental pv/NkT vs. reduced density for $N_2$.

APPROVED FOR PUBLIC RELEASE

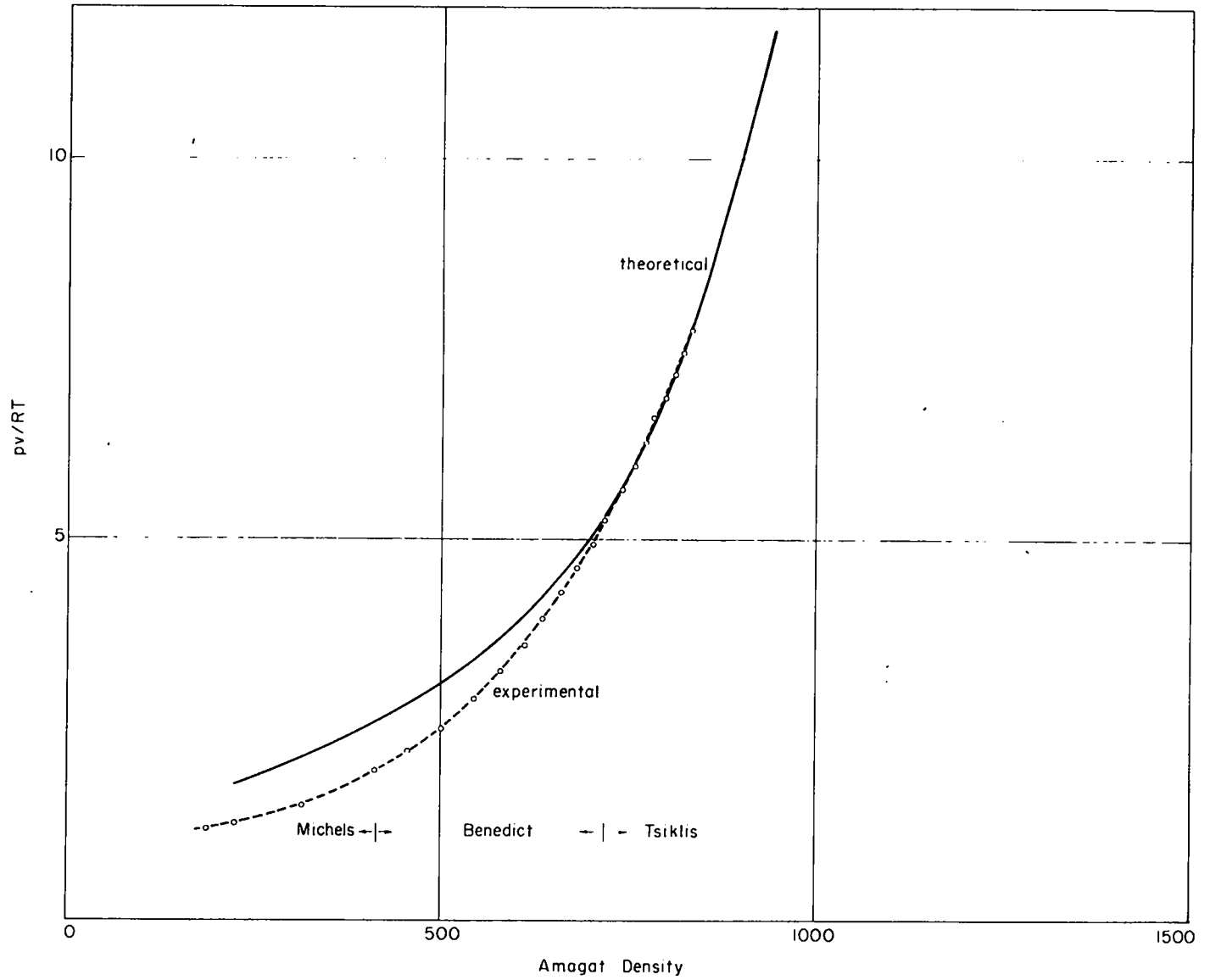


Figure 6. Theoretical and experimental pv/RT vs. Amagat Density for $N_2$.

only a single rough calculation for the reaction $H_2O + CO \rightarrow H_2 + CO_2$. Under conditions approximating the C-J point for RDX at 1.6 g/cm$^3$ loading density it was found that the equilibrium lay far to the left, with entirely negligible amounts of $H_2$ and $CO_2$. In this calculation the L-J parameters of Bird and Spotz[7] were used to compute the $\sigma_{ij}^*/\bar{v}^*$ and $\Lambda_{ij}^*/\bar{\Lambda}^*$, while the values of $\tau$ and $\Theta$ were approximately those for $N_A \bar{\epsilon}^* = 200$ cal/mole, $\bar{v}^* = 20.65$ cm$^3$/mole. We plan to make a more extensive investigation of the various possible equilibria in the near future.

A comparison of the ordinary L.J.D. free volume equation of state with low temperature, static high pressure measurements on $N_2$ is also of interest. Such a comparison was made by Wentorff, et.al.[2,8], but they did not use all the available experimental data[9]; in addition new data up to 10,000 atm. has recently appeared[10]. The older measurements of Bridgman[11] are apparently in error[9,10]. We have made a qualitative graphical comparison, shown in Figures 5 and 6. In Figure 5 we have chosen, as in Figure 1, $\tau^{-1}$ as the independent variable, and have plotted various theoretical L.J.D. isotherms of $\delta^*$. The experimental isotherm chosen was for 150°C; with $\tau^{-1}$ as independent variable it becomes a family of curves with parameter v*. We seek a coincidence of two curves, one from each of the two families. The values $\epsilon^*/k = 92°K$, $v^* = 31.2 \frac{cm^3}{mole}$

---

[7]Bird and Spotz, University of Wisconsin Report CM-599, 1950; NOrd 9938; WIS-I-C.

[8]Michels, Wouters and de Boer, Physica, 3,585 (1936)

[9]M. Benedict, J. Am. Chem. Soc.,59,2224 (1937); ibid.,39,2233 (1951)

[10]D. S. Tsiklis, Dokl. Akad. Nauk. U.S.S.R.,79(2),289-90 (1951)

[11]P. W. Bridgman, Proc. Am. Acad. Arts Sci.,70(1), (1935)



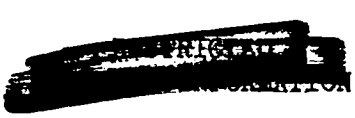

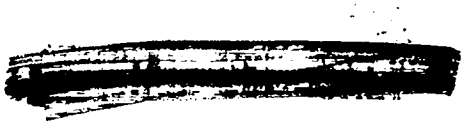

are seen to result in rather good agreement for $\gamma^{-1} > 1.0$, with increasing disagreement at lower densities, the theoretical values of $\mathcal{P}$ being too high. It is not possible to choose values outside this neighborhood which will give agreement over any appreciable interval in $\gamma^{-1}$. The values quoted are in rather good agreement with the values 91.5°K and 30.0 $cm^3$/mole found from viscosity measurements, and with the values 95.0°K and 30.5 $cm^3$/mole derived from second virial coefficient measurements[7]. One interpretation is that the L-J potential is possibly a good representation of the $N_2$ intermolecular potential over the corresponding range of intermolecular distances, the discrepancy at low density being due to the failure of one or more approximations in the theory. In Figure 6 the experimental and theoretical values of $T$ are plotted against Amagat density, using the values $\epsilon^*/k$ = 91.5°K, v* = 31.2 $cm^3$/mole for the theoretical curve.

One is naturally led to inquire whether or not a correspondence can be set up which relates the experimental detonation region of temperature and density to a section of the low temperature isotherm of Figures 5 and 6. For a discussion of the validity of the theoretical approximations, an attempt to select values of temperature and volume such that the cell potential divided by $kT$ is approximately the same function of the reduced cell radius r/a seems appropriate. That this should be possible, at least for high densities and under the assumption of the L-J potential, is suggested by the fact that for small $T$ the $T^{-4}/\theta$ term in

$$\frac{W(r)}{kT} = 12\left[\frac{T^{-4}}{\theta} l\left(\frac{r^2}{a^2}\right) - 2\frac{T^{-2}}{\theta} m\left(\frac{r^2}{a^2}\right)\right]$$

will dominate, being assisted also by the dominance of $l(r^2/a^2)$ over $m(r^2/a^2)$. Consequently $\frac{W(r)}{kT}$, $\mathcal{P}$, and $\mathcal{E}'/\theta$, to a certain approximation, may be expected to depend on the single variable $T^{-4}/\theta$.

By actual computation of w(r)/kT we find that such a correspondence can indeed be set up, with values in the neighborhood of those predicted by the preceding argument. Although admittedly rough it is believed that the argument has semi-quantitative validity. As a result we find that the upper limit of the detonation region ( $\rho_o$ = 1.8 g/cm$^3$) corresponds to an Amagat density of 810 in Figure 5, while the lower limit (taken to be 0.8 g/cm$^3$) corresponds to density 400. It is interesting that the corresponding point of the upper limit occurs in the region of good agreement between experiment and theory, while for the lower limit, it is well into the region of disagreement. The suggestion is that if multiple occupancy, for instance, is important in the latter region at 150°C, then it may also be of importance in the lower loading density range in detonation. Conjectures about its importance in the former case have been made by others[2]. It should be noted that this discussion assumes, rather than proves or indicates, the validity of the L-J potential. Rather different intermolecular distances are in question in the two cases, and it is conceivable that at least part of the discrepancy in the detonation case may be due to this.

To date we have made only an exceedingly rough estimate of the departure from single occupancy, following the procedure of Janssens and Prigogine[12]. A very appreciable effect on $\mathcal{H}$ and $\mathcal{E}'$ for $\theta$ and $\tau$ near the lower limit of the loading density range was indicated. A more thorough investigation of this point will be made.

If, as may be suspected from the preceding discussion, multiple

---

[12] P. Janssens and I. Prigogine, Physica 16, 895-906 (1950)





occupancy is becoming important in the lower loading density region, then it is also likely that the basic delta-function approximation to the molecules configurational distribution function $\varphi(r)$ in the cell may be breaking down at somewhat higher loading densities. Kirkwood[13] has suggested an iterative scheme of obtaining higher approximations to $\varphi(r)$, and we hope to investigate this point.

We also intend to examine the possibility of utilizing multiple occupancy as a conceptual tool in extending the present theory to molecules of different sizes.

In order to obtain numerical results from the theory in the region of present interest, it is necessary to specify the potential of intermolecular force for values of $r/r_o$ covering a range of about one-half to two. The presently available experimental information gives little more than a rough indication of the form of the potential in the high-energy part of this range.

The choice of the Lennard-Jones form for the intermolecular potential was made largely for the sake of mathematical convenience. The (6, 12) form has been used previously in this type of work, although present experimental evidence provides little, if any, reason for preferring it to the (6, 9) form.

The intermolecular potential of helium has probably been investigated more thoroughly than that of any other substance. Figures 7 and 8 show some of the proposed potential functions, both theoretical and experimental. The second virial coefficient of helium has recently been measured to 1200°C by Yntema and Schneider[14]. They attempted to determine from their data the

---

[13] J. G. Kirkwood, J. Chem. Phys. 18, 380-2 (1950)

[14] J. L. Yntema and W. G. Schneider, J. Chem. Phys., 18, 641 and 646 (1950)

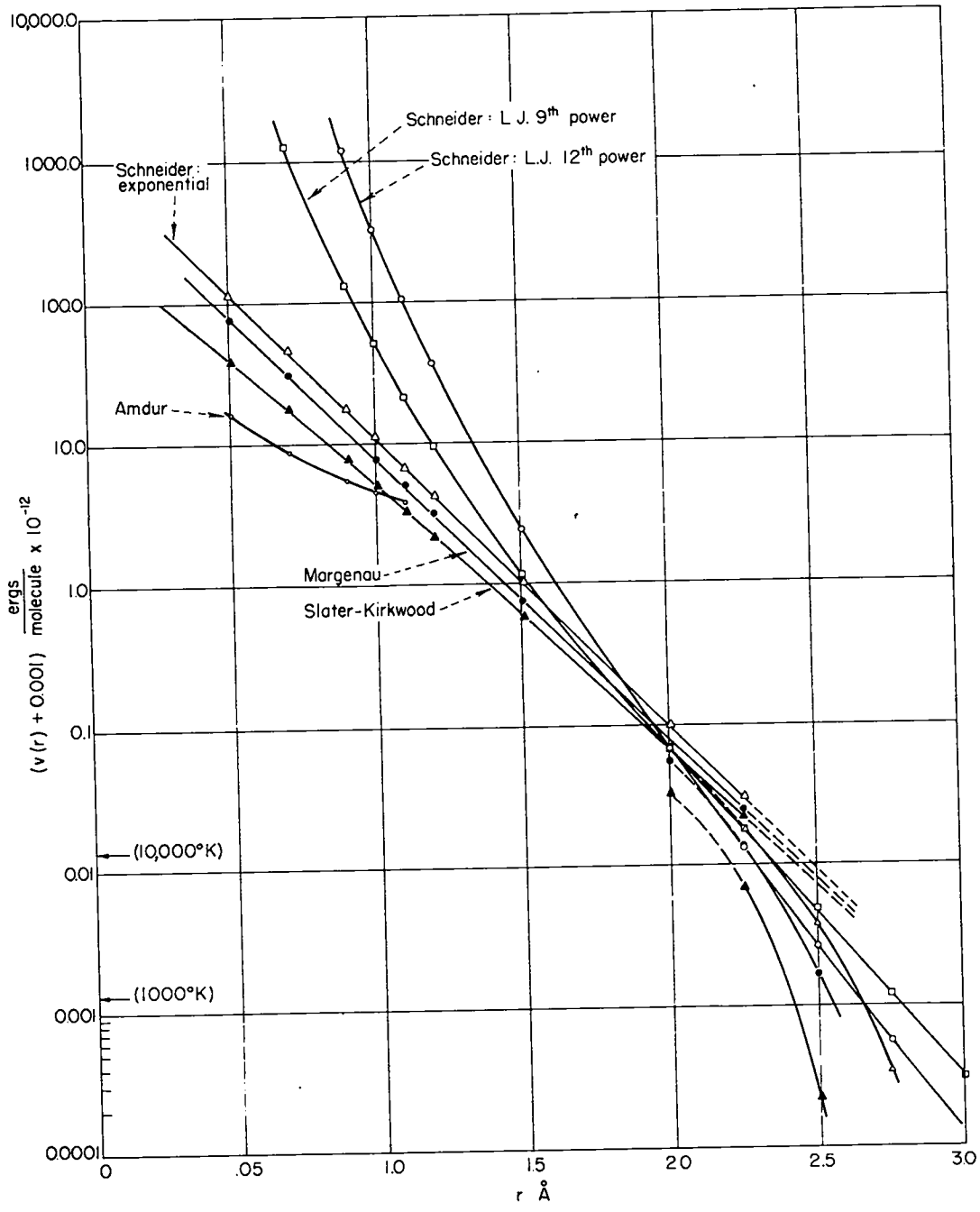


Figure 7. Potential energy curves for helium at distances less than $r_o$. For potentials with exponential repulsion, the portions of the curves above the break represent the repulsive terms only.

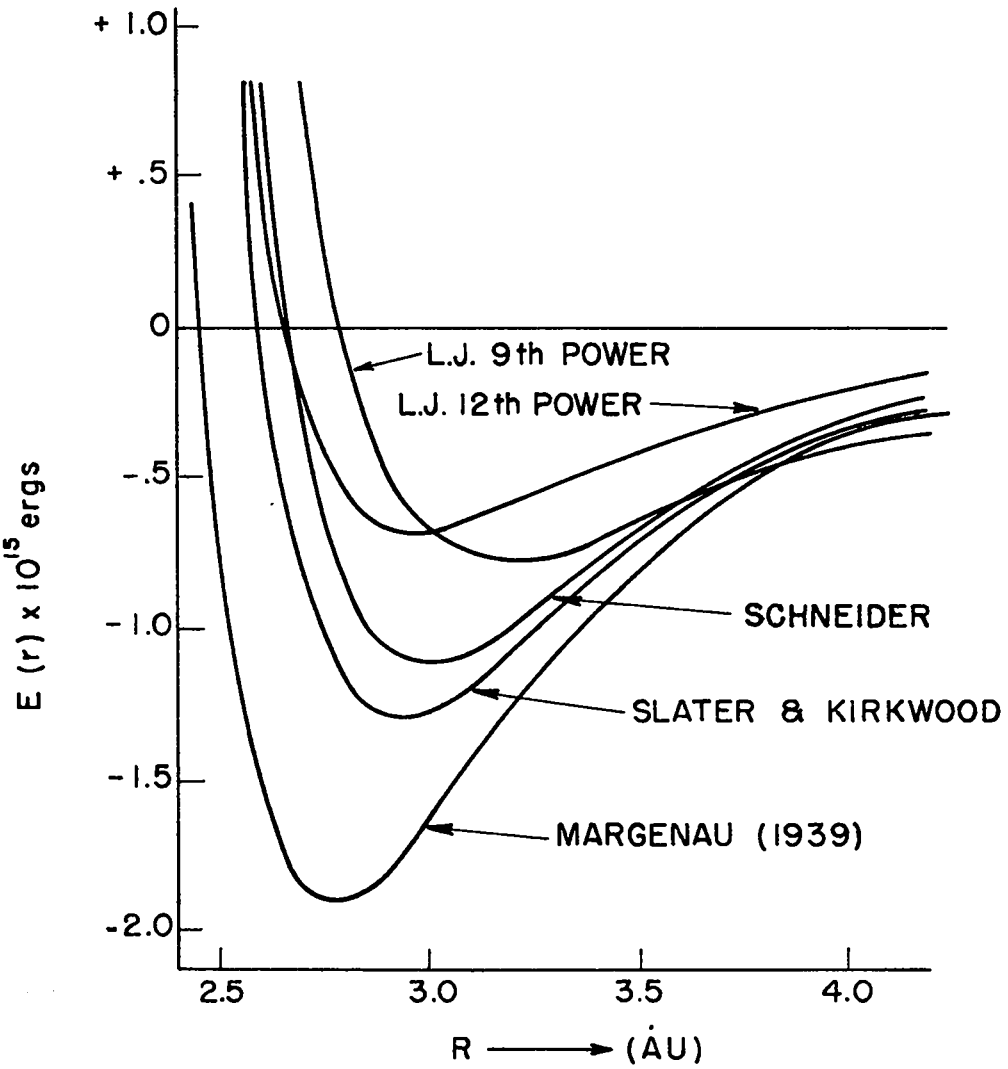


Figure 8. Potential energy curves for helium in the neighborhood of the minimum.[14]

as well as those in a form with exponential repulsion:

$$V(r) = b\,e^{-r/\rho} - \frac{c_1}{r^6} - \frac{c_2}{r^8}$$

The results indicated some preference for the exponential form, which could be made to reproduce the experimental second virial coefficient fairly well over the entire temperature range, although a divergence just exceeding the experimental error at the highest temperature suggests that the fit would become progressively poorer at higher temperatures. Of the two Lennard-Jones forms, a slight preference for the (6, 9) was indicated.

Margenau[15] and Slater and Kirkwood[16] have carried out quantum-mechanical calculations of the helium potential. Slater and Kirkwood calculate the repulsive term from first-order perturbation theory, then add an attractive term resulting from dispersion forces. Margenau[15] asserts that this type of approach is somewhat inconsistent, inasmuch as the repulsive force is calculated from first-order perturbation theory on wave-functions satisfying the Pauli exclusion principle, while the attractive force is calculated from second-order perturbation theory on wave-functions not satisfying the Pauli principle. Thus the attractive and repulsive terms calculated in this way may not be simply additive. His treatment claims consistency in this respect, for it uses a single set of wave-functions satisfying the Pauli principle and carries the perturbation treatment to second-order. His treatment claims reasonable validity at the minimum, but there is some doubt as to the validity of some of the later approximations at smaller distances.

The intermolecular potential at very small intermolecular distances

---

[15] H. Margenau, Phys. Rev., 56, 1000 (1939)

[16] J. C. Slater and J. Kirkwood, Phys. Rev., 37, 682 (1931)

has been determined from measurements of He-He collision cross-sections[17]. As shown in Figure 7, it lies somewhat below the other potentials, and has a somewhat different shape. This information is of no direct use to us, however, since it does not extend to sufficiently large intermolecular distances.

The curves presented in Figures 7 and 8 indicate that the intermolecular potential of the simplest rare gas is not well determined even in the neighborhood of the minimum, which exerts a considerable effect on the second virial coefficient at ordinary temperatures.

Figure 9 illustrates, in a rough way, the portion of the potential function which is important in determining the thermodynamic properties of the system. The two marked values for each $T$ and $\Theta$ indicate the ranges of intermolecular distance covered in the cell integration when $G$, $g_L$, and $g_M$ have reached approximately 90% or 99% of their final values. The pairs of values of $T$ and $\Theta$ given in Figure 9 correspond to the four corner pairs of values of $T$ and $\Theta$ in our double entry tabulation of the reduced equation of state.(Tables 1-6) The ranges of $T$ and $\Theta$ covered in the detonation calculation can be found in Table 7. In considering the implications of Figure 9 with respect to the importance of the shape of the potential function it must be remembered that the contribution to the compressibility, $\mathcal{Z}$, of terms containing the integrals $G$, $g_L$, and $g_M$, depends markedly on the values of $T$ and $\Theta$. The compressibility is given by

$$\mathcal{Z} = \left\{ 1 - \frac{12}{\Theta}\left[2.4090\,T^{-2} - 2.0219\,T^{-4}\right] - \frac{48}{\Theta}\left[T^{-2} g_M/G - T^{-4} g_L/G\right]\right.$$

[17] I. Amdur, D. E. Davenport, and M. C. Kells, J. Chem. Phys., 18, 525 (1950)

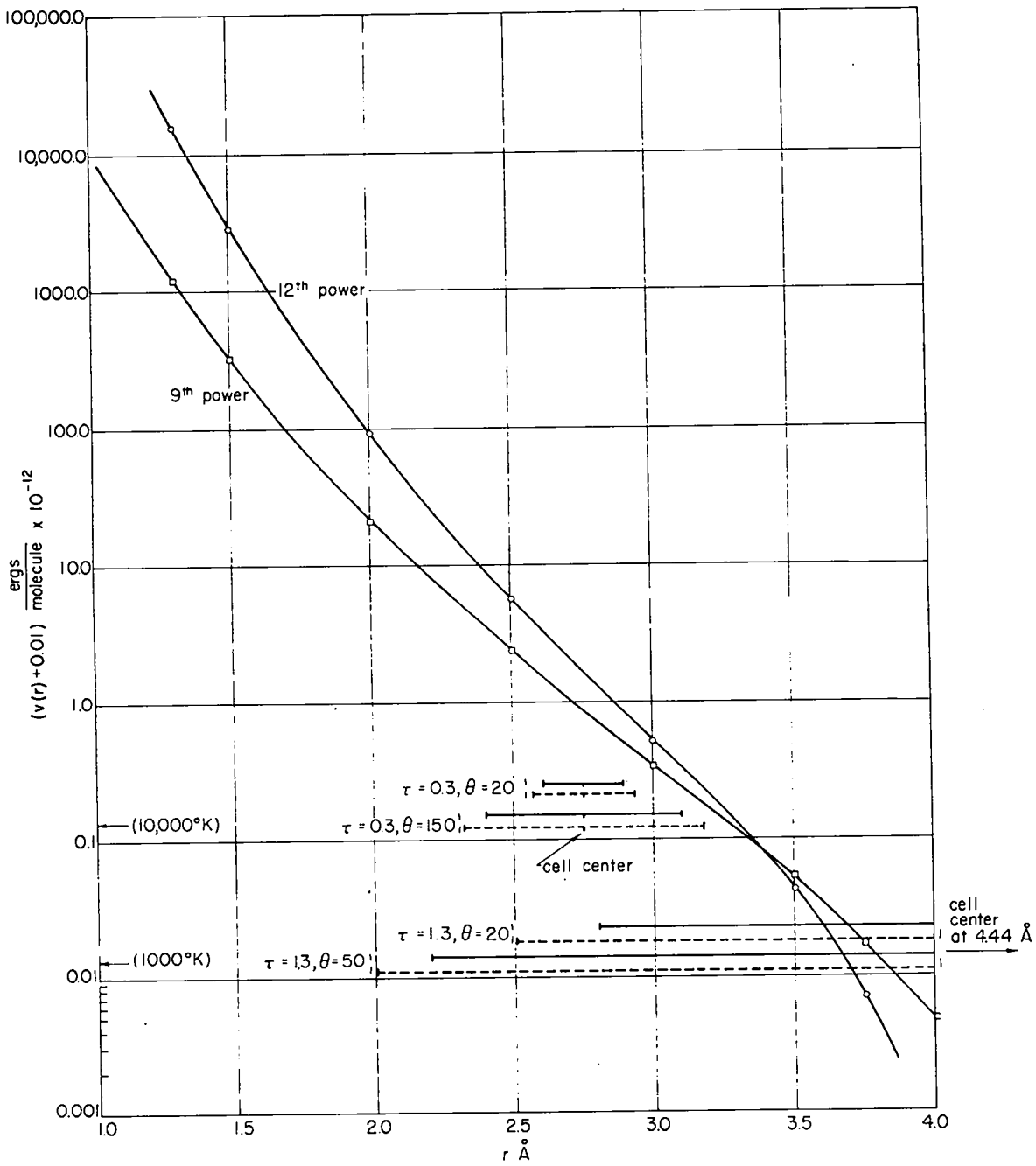


Figure 9. Lennard-Jones potential energy curves for nitrogen showing the intervals of intermolecular distance determining the thermodynamic properties.

For $\tau = 0.3$, $\theta = 20$ the term containing the integrals contributes about 10% of the value of $\mathcal{H}$; for $\tau = 1.3$, $\theta = 150$ the contribution of this term is well above 50% of the final value. The situation is complicated by the presence of the second term. For the low density-high temperature portion of the region covered by our tables, the integrations extend over wide ranges of internuclear distance and $\mathcal{H}$ is dominated by the third term. For high densities and low temperatures the second term, which is related to the energy of the molecule at the center of the cell, dominates; the third, which takes into account both the energy of the molecule at the center of the cell and what might be described as the "local shape" of the potential, is relatively unimportant. Thus the form of the potential and the values of its parameters influence the result in a rather complicated way. The situation with regard to the imperfection energy $\epsilon'$ is similar.

Because of the manifest uncertainty in the potential function, we plan to carry out calculations of the equation of state for the Lennard-Jones (6, 9) form, and probably also for a potential function of the form $V(r) = \left(\frac{6}{\alpha-6}\right)(\epsilon)\left[e^{-\alpha\left(\frac{r}{r_0}-1\right)} - \frac{\alpha}{6}\left(\frac{r_0}{r}\right)^6\right]$. The equation of state from the latter potential function would be a function of the reduced variables $\theta$ and $\tau$, defined as before, but would depend in addition on the value of the non-dimensional parameter $\alpha$. We have written down the expressions for the integrals analogous to $G$, $g_L$, and $g_M$; the labor involved in the numerical integration for a given value of $\alpha$ appears to be about twice that which is required for the Lennard-Jones potential.

Because we expect the new data for RDX in the high density region to be available shortly, we have not yet considered the extension to other conventional explosives. Should substantial agreement be obtained for the former, we shall of course proceed to such an application.



[redacted]